Decay rates of *N*-electron resonant states in a double-barrier quantum dot under the influence of electric and magnetic fields

W. Y. Ruan[1,2] and Yia-Chung Chang[1]
[1]*Department of Physics and Materials Research Laboratory, University of Illinois at Urbana-Champaign, Urbana, Illinois 61801*
[2]*Department of Applied Physics, South China University of Technology, Guangzhou 510641, People's Republic of China*
(Received 22 April 2002; published 4 October 2002)

Resonant energies and decay rates of interacting electrons in a double-barrier quantum dot subjected to parallel electric and magnetic fields are investigated via a complex coordinate rotation method. We show that the decay rate increases monotonically with the electric field, but changes discontinuously with the magnetic field. The discontinuous jumps correspond to changes in the orbital angular momentum and spin.

DOI: 10.1103/PhysRevB.66.155311 PACS number(s): 72.20.−i, 71.45.Gm, 73.21.La, 73.40.Gk

Resonant tunnelings through double-barrier semiconductor quantum dots, driven by a bias voltage, are highly sensitive to the electronic structures of the dots. Experiments conducted on these devices, so-called single-electron transistors (SET's), to date have yielded rich data,[1–3] the full understanding of which requires a quantum-mechanical treatment of the electron-electron (*e-e*) interactions and the effects of external fields. To our knowledge, the existing theoretical investigations of quantum dot transport properties are all based on the tunneling Hamiltonian approach.[4–6] In this paper, we report our first-principles calculations of the lifetimes of quasibound states (resonances) of a double-barrier confined quantum dot. For convenience in calculation, the system is embedded in a quantum wire, so the motion in the *x-y* plane is quantized both inside and outside the quantum dot. However, many interesting predictions obtained by this model should remain qualitatively valid for a quantum dot sandwiched between planar junctions as in typical experimental setups for SET's. To emphasize the effects of *e-e* interactions and external fields, we consider systems in which the strengths of *e-e* interactions and external fields are comparable with the barrier heights. We demonstrate that a combination of the *e-e* interactions and a varying magnetic field can lead to dramatic changes in the tunneling rates. Overall, the magnetic field tends to suppress the tunnelings of interacting electrons, in agreement with the experimental observation by Ashoori *et al.*[7]

For the calculations of *N*-electron resonances ($N>1$), the traditional phase-shift analysis[8,9] and the complex-energy methods[10] are not applicable due to the unavailability of exact *N*-body wave functions. The stabilization-diagram approach[11] is computationally too demanding, and its applicability in the region of strong electric fields is problematic.[12] In this paper, we employ the complex coordinate rotation (CCR) method, which emerged about 30 years ago and has been successfully applied to some atomic resonances.[13] The original CCR method, its mathematical arguments from the spectrum theory of operators[14–16] and its hitherto applications have relied on a complex rotation of the same angle α for all coordinates, i.e., $(x_j,y_j,z_j) \rightarrow (e^{i\alpha}x_j, e^{i\alpha}y_j, e^{i\alpha}z_j)$ $(j=1,...,N)$. This global rotation of coordinates is most suitable for spherically symmetric systems, such as atomic systems in which the particles interact via the isotropic Coulumb potentials $1/r$,[17] but is unsuitable for anisotropic systems such as the quantum dots to be studied in this paper, because of its extremely slow convergence. Here we generalize this method and point out that the resonant states of a system can be obtained by a more general complex coordinate rotation $(x_j,y_j,z_j) \rightarrow (e^{i\alpha_{xj}}x_j, e^{i\alpha_{yj}}y_j, e^{i\alpha_{zj}}z_j)$, which allows us to avoid unnecessary computation requirements by optimizing the parameters $\{\alpha_{\mu j}|\mu=x,y,z;j=1,...,N\}$,[18] since the wave functions of an anisotropic system can be extended more in some directions than in others. Under a CCR, the Hamiltonian H of a system becomes a non-Hermitian operator $\overline{H}$. For sufficiently large $\alpha_{\mu j}$ in the domain $0\leqslant\alpha_{\mu j}\leqslant\pi/2$, the spatially extended wave function $\Psi_{\rm res}$ of a resonant state becomes a square-integrable function $\overline{\Psi}_{\rm res}$. Hence the resonant states and the associated energies and lifetimes can be obtained by diagonalizing the rotated Hamiltonian $\overline{H}$ in a model space spanned by discrete, square-integrable basis functions. The spatial wave function $\Psi_{\rm sc}$ of a scattering state is rotated into another extended function $\overline{\Psi}_{\rm sc}$, the expansion of which in terms of discrete, square-integrable basis functions would diverge. After the diagonalization, the resonant states can be identified from the spectrum $\{\overline{\zeta}_1,\overline{\zeta}_2,...,\overline{\zeta}_n,...\}$ of $\overline{H}$ by implementing the stabilization conditions $\partial\overline{\zeta}_n/\partial\alpha_{\mu j}=0$, or by changing the number of basis functions. The complex eigenenergy $\overline{\zeta}_n$ associated with a resonant state can be written as $\overline{\zeta}_n=(\epsilon_n,-\Gamma_n/2)$, in which the real part ϵ_n is the resonant energy, Γ_n is the decay rate ($\hbar/\Gamma_n$ gives the lifetime).

The quantum dot model considered here has two symmetric barriers along the transport (z) direction, sandwiching a potential well at $z=0$, which is parametrized as a sum of two Gaussian functions,

$$v(z)=v_{01}e^{-z^2/a_1^2}+v_{02}e^{-z^2/a_2^2}. \tag{1}$$

The parameters can be tailored to match the quantum dot systems used in actual experiments. The numerical results presented in this paper are for $v_{01}=-61$ meV, $v_{02}=30$ meV, $a_1=12$ nm, and $a_2=30$ nm, which are so chosen as to support a bound state similar to the experimental device described in Fig. 3 of Ref. 2. The barrier height (see Fig. 1) is of the same order as the strength of *e-e* interactions in the

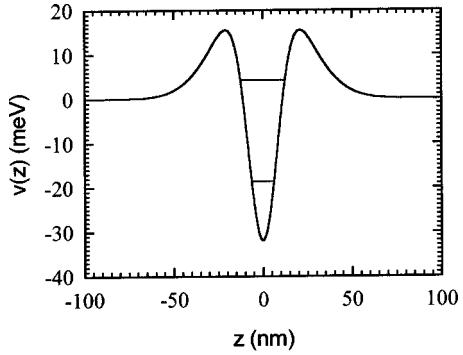

FIG. 1. Double-barrier potential along the tunneling direction. The horizontal lines give the two lowest states supported by the potential, the ground state is a bound state, the first excited state is a resonant state.

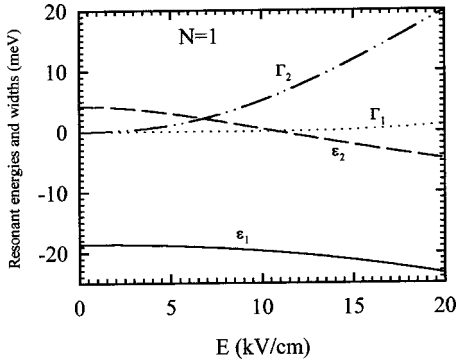

FIG. 2. The resonant energies and decay rates of the two lowest resonant states of $h(z)$ as a function of electric-field strength, E.

dot so that the tunneling rates will be significantly enhanced by the *e-e* repulsions. Similar to the systems considered in Refs. 19 and 20, the confinement potential in the *x-y* plane, for all *z*, is approximated by a parabolic potential $\frac{1}{2}m_e^*\omega_0^2\rho^2$, with $\rho=(x^2+y^2)^{1/2}$. The electric (E) and magnetic (B) fields are oriented parallel to the z direction. The single-electron Hamiltonian separates, $h(\mathbf{r})=h(x,y)+h(z)$,

$$h(x,y)=-\frac{1}{2m_e^*}(\mathbf{p}+e\mathbf{A})^2+\tfrac{1}{2}m_e^*\omega_0^2\rho^2+g_e^*\mu_B B\hat{S}_z, \tag{2}$$

$$h(z)=-\frac{\hbar^2}{2m_e^*}\frac{\partial^2}{\partial z^2}+v(z)+eEz, \tag{3}$$

where m_e^* is the effective mass of the electron, $A=(\mathbf{B}\times\mathbf{r})/2$ is the vector potential of the magnetic field, g^* is the effective g factor, μ_B is the Bohr magneton. Obviously $h(\mathbf{r})$ describes the motion of an electron in a double-barrier quantum dot embedded in a quantum wire. We ignore the electron mass difference between the dot and the barrier materials. The eigenequation of operator $h(x,y)$ is exactly solvable, yielding

$$\phi_{nl}(\vec{\rho})=\left[\frac{2n!}{a^2(n+|l|)!}\right]^{1/2}(\rho/a)^{|l|}L_n^{(2|l|)}(\rho^2/a^2)e^{-\rho^2/2a^2}\frac{e^{il\varphi}}{\sqrt{2\pi}}, \tag{4}$$

$$\epsilon_{nl}=(2n+|l|+1)\hbar\omega-l\frac{\hbar\omega_c}{2}+g_e^*\mu_B B s_z, \tag{5}$$

where $a=(\hbar/\omega m_e^*)^{1/2}$ is the effective magnetic length, $\omega_c=eB/m_e^*$ is the cyclotron frequency $\omega=(\omega_0^2+\omega_e^2/4)^{1/2}$, $L_n^{(2|l|)}$ are Laguerre polynomials. The nontrivial problem is to find out the resonant states of $h(z)$. We diagonalize the rotated Hamiltonian $(e^{i\alpha}z)$ in the model space spanned by the one-dimensional (1D) oscillator harmonics,

$$F_k(z)=\left[\frac{1}{\beta\pi^{1/2}2^k k!}\right]^{1/2}H_k[(z-z_0)/\beta]e^{-(z-z_0)^2/2\beta^2}, \tag{6}$$

where $\beta=(\hbar/m_e^*\Omega)^{1/2}$, H_k are Hermite polynomials. The equilibrium point z_0 of the oscillator is determined by $d[v(z)+eEz]/dz=0$, and the oscillator frequency by

$$\Omega=\left\{\frac{1}{m_e^*}\frac{d^2[v(z)+eEz]}{dz^2}\right\}_{z=z_0}^{1/2}.$$

We estimate the accuracy of the calculated complex eigenenergies by varying the parameter α and the number of basis functions used. For example, using 51 harmonics with $|k|\leqslant 25$ and setting the electric field to $E=20$ kV/cm yield a ground- (resonant) state eigenenergy $\overline{\zeta_1}=(-23.467251, -0.56897935)$ meV, which remains unchanged (up to eight significant digits of both its real and imaginary parts) with α varied in the range of $\pi/60\leqslant\alpha\leqslant\pi/4$. When the number of basis functions is further increased, the calculated complex eigenenergies of resonant states become even less sensitive to the variation of α. If we take α to be the optimum value $\alpha_{\rm op}\approx\pi/8$, the number of basis functions can be reduced to 31, while maintaining the same accuracy. In our calculations, although $\alpha_{\rm op}$ is found to vary with E, there is no noticeable deterioration of convergence due to increasing E. For $\alpha>\pi/4$, since the rotated potential $v(e^{i\alpha}z)=v_{01}e^{-(\cos 2\alpha+i\sin 2\alpha)z^2/a_1^2}+v_{02}e^{-(\cos 2\alpha+i\sin 2\alpha)z^2/a_2^2}$ oscillates with ever increasing amplitudes as $z\to\pm\infty$, the convergence slows down significantly with increasing α. Figure 2 exhibits the resonant energies and decay rates of the two lowest resonant states of $h(z)$ as a function of E. The energies of the resonant states decrease quadratically with increasing E, displaying a second-order Stark effect, while the decay rates (or resonant widths) increase monotonically, with the higher-lying state much more susceptible to the electric field. Other resonant states lie beyond the scope of the figure.

We now consider N interacting electrons in the dot. The Hamiltonian reads

$$H=\sum_{i=1}^{N}h(\mathbf{r}_i)+\frac{e^2}{4\pi\epsilon}\sum_{i>j}^{N}\frac{1}{(\rho_{ij}^2+z_{ij}^2)^{1/2}}. \tag{7}$$

An important feature of Eq. (7) is that the (x, y) motion and the z motion are now coupled via the *e-e* interactions. Hence unlike a single-electron dot, the tunneling of N electrons will be tuned by the magnetic field. We diagonalize the rotated

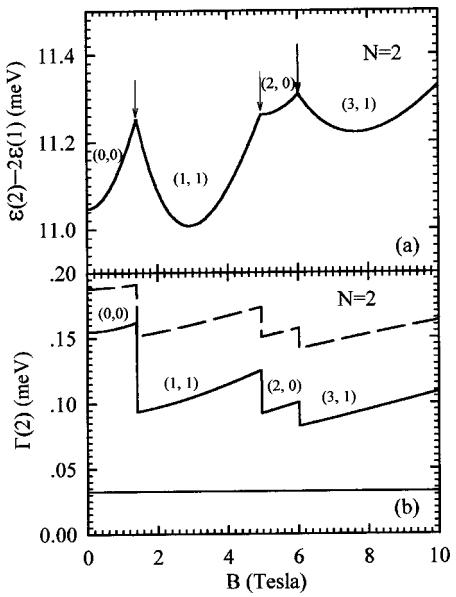

FIG. 3. (a) Resonant energy of the ground state as a function of the magnetic-field strength for $N=2$. The arrows point to locations where a switching in orbital angular momentum L and spin S occurs. The numbers in the brackets give (L,S). (b) Decay rate (solid curve) and averaged Coulumb energy divided by a factor 50 (dashed curve) as functions of the magnetic field. The horizontal line gives the decay rates in the absence of the *e-e* interactions.

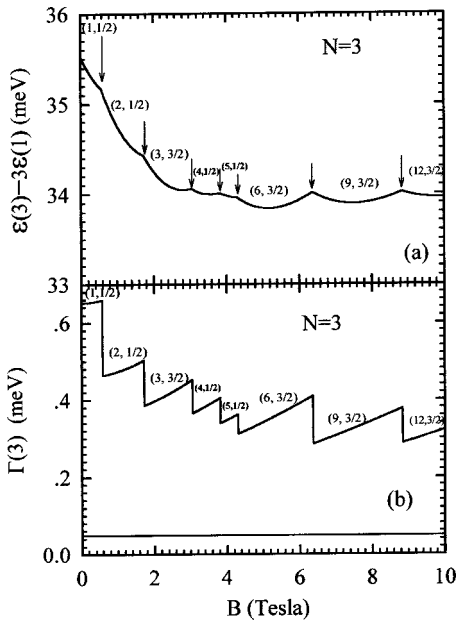

FIG. 4. (a) Resonant energy of the ground state as a function of the magnetic-field strength for $N=3$. (b) Decay rate as a function of the magnetic field. The horizontal line gives the decay rates in the absence of the *e-e* interactions.

Hamiltonian $\bar{H}$ to obtain the resonant states as before. The antisymmetric basis functions we use are Slater determinants composed of single-particle basis functions, each of which is the product of a 2D oscillator harmonics [given by Eq. (4)], a 1D oscillator harmonics [given by Eq. (6)], and an electron spinor. The complex rotation angles $(\alpha_{xj},\alpha_{yj},\alpha_{zj})$ are independent of j owing to the identity of electrons, the optimum values of which turn out, from our numerical calculations, to have $\alpha_x=0$ and $\alpha_y=0$. This is understandable since there is no wave-function leakage along the x and/or y directions. The only nonvanishing α_z depends on the field strengths. Approximately, the convergence is 13^{N-1} times faster than the global CCR of assuming $\alpha_x=\alpha_y=\alpha_z=\alpha$ for the present cases.

Figures 3 and 4 exhibit the resonant energies and decay rates of $N=2$ and 3 in their ground states. They have been calculated using parameters appropriate for GaAs and a value of 3.6 meV for $\hbar\omega_0$, and the electric-field strength $E=10$ kV/cm. The effect of a varying electric field on the N-electron resonances is qualitatively similar to that of $N=1$ reported above, except that the *e-e* interactions further enhance the decay rates. Here we focus on the effect of a varying magnetic field on the resonant tunneling through the ground state (i.e., tunneling at zero temperature). Since the *e-e* interactions conserve the total azimuthal angular momentum L and the total spin S, we use them to label the eigenstates. The resonant energies of few electrons in a quantum dot in a magnetic field have been calculated by several authors by treating the systems as bound-state problems.[19–24] In the case of $N>1$, there are typically several tunneling processes. Γ represents the total decay rate via all processes.

The application of magnetic field brings about an important change to the single-particle wave functions in the x-y plane [see Eq. (4) and the subsequent definition of magnetic length a]. States of all l shrink in radius as the magnetic field is increased. Hence the average spacing between electrons tends to decrease with increasing B. To avoid being compressed to a point at the dot's center, the electrons transit to states of higher l values at certain critical B values at which the transitions can occur without causing any increase in the total energy (i.e., level crossings),[25–27] thereby a series of kinks develop in the resonant energies [see Figs. 3(a) and 4(a)]. In each of these transitions, a sudden increase in the kinetic and confinement energies is accompanied by a sudden drop of the same amount of Coulumb energy. For $N=2$, the energetically most favorable configuration is for the electrons to be on the opposite sides and their centers of mass located at the potential minimum point $(0,0,z_0)$, in which a rotation of π about the z axis is equivalent to the exchange of the two electrons, i.e., $R(\pi)\Psi_0=P_{12}\Psi_0$, where Ψ_0 is the probability amplitude of the configuration. However, $R(\pi)\Psi_0=e^{iL\pi}\Psi_0$ and $P_{12}\Psi_0=(-)^S\Psi_0$ leads to $[e^{iL\pi}-(-)^S]\Psi_0=0$. In other words, the nodeless ground states can occur only when $L+S=$even. Applying the similar arguments to $N=3$ leads us to the conclusion that the nodeless ground state occurs when L is a multiple of 3 ($L=3,6,9,12,...$) for $S=\frac{3}{2}$ and when L is not a multiple of 3 ($L=1,2,4,5,7,...$) for $S=\frac{1}{2}$. All the ground states in Figs. 3 and 4 obey these rules. In low magnetic field, both the spin polarized and spin unpolarized states compete to be the ground state. Due to the presence of the Zeeman term, the spin unpolarized states have shorter ranges of magnetic-field strength to form the ground state than the spin polarized

states in intermediate magnetic field, and are completely excluded from forming the ground state in high magnetic field.

There is a simple way to interpret the sawtooth structures of the decay rates exhibited in Figs. 3(b) and 4(b). The interacting electrons can be thought of as a droplet of incompressible liquid. A shrink (expansion) of its size in the *x-y* plane brings about an expansion (shrink) of its size in the *z* direction, and vice versa. Since the tunneling rate depends on the amount of wave-function leakage through the barriers separating the dot from the leads, it varies in much the same way as the Coulumb energy [see Fig. 3(b)] in a varying magnetic field.

With the application of magnetic field there is another important change in the single-particle states. States with the same Landau-level index, $[n+(|l|-l)/2]$, but with different l tend to be degenerate to form Landau levels [see Eq. (5)]. The single-particle energy difference between states $l+1$ and l, $\hbar[(\omega_0^2+\omega_c^2/4)^{1/2}-\omega_c/2]$, tends to vanish as $B\rightarrow\infty$. It becomes energetically less costly to transit to a higher l orbital as the magnetic-field strength is increased. Consequently, the spacing between electrons gains a net increase and the decay rate gains a net decrease from each transition. This elucidates a previous unexplained phenomenon observed in Ref. 7.

In conclusion, we have investigated the transport properties of a quantum dot containing a few electrons and coupled to leads through soft barriers using a generalized CCR method. We show that the *e-e* interactions and an external magnetic field cause discrete changes of the tunneling rates.

The authors acknowledge the many helpful discussions with Dr. David M. T. Kuo and Dr. Ge-Fei Qian. This work was supported by a subcontract from the University of Southern California under the MURI program, AFOSR, Contract No. F49620-98-1-0474. The work of W.Y.R. was also supported in part by the National Natural Science Foundation, Grant No. 90103028, People's Republic of China.

[1] R. C. Ashoori, Nature (London) **379**, 413 (1996).
[2] L. P. Kouwenhoven, D. G. Austing, and S. Tarucha, Rep. Prog. Phys. **64**, 710 (2001).
[3] T. Schmidt, M. Tewordt, R. H. Blick, R. J. Haug, D. Pfannkuche, and K. v. Klitzing, Phys. Rev. B **51**, 5570 (1995).
[4] J. M. Kinaret, Y. Meir, N. S. Wingreen, P. A. Lee, and X. G. Wen, Phys. Rev. B **46**, 4681 (1992).
[5] W. Hofstetter and H. Schoeller, Phys. Rev. Lett. **8801**, 6803 (2002).
[6] P. G. Silvestrov and Y. Imry, Phys. Rev. B **65**, 035309 (2002).
[7] R. C. Ashoori, H. L. Stormer, J. S. Weiner, L. N. Pfeiffer, K. W. Baldwin, and K. W. West, Phys. Rev. Lett. **71**, 613 (1993).
[8] E. J. Austin and M. Jaros, Phys. Rev. B **31**, 5569 (1985).
[9] Y. Guo, B. L. Gu, and W. H. Duan, Z. Phys. B: Condens. Matter **102**, 217 (1997).
[10] D. Ahn and S. L. Chuang, Phys. Rev. B **34**, 9034 (1986).
[11] V. A. Mandelshtam, T. R. Ravuri, and H. S. Taylor, Phys. Rev. Lett. **70**, 1932 (1993).
[12] D. M. T. Kuo and Y. C. Chang, Phys. Rev. B **61**, 11 051 (2000).
[13] Y. K. Ho, Phys. Rep. **99**, 1 (1983).
[14] J. Aguilar and J. M. Combes, Commun. Math. Phys. **22**, 269 (1971).
[15] E. Balslev and J. M. Combes, Commun. Math. Phys. **22**, 280 (1971).
[16] B. Simon, Commun. Math. Phys. **27**, 1 (1972).
[17] If the Hamiltonian of a Coulumb system is $H=T+V$, the rotated Hamiltonian will be $\bar{H}=e^{-2i\alpha}T+e^{-i\alpha}V$, facilitating the evaluation of matrix elements.
[18] The mathematical arguments and a comparison with other methods will be presented elsewhere.
[19] P. A. Maksym and T. Chakraborty, Phys. Rev. Lett. **65**, 108 (1990).
[20] P. Hawrylak and D. Pfannkuche, Phys. Rev. Lett. **70**, 485 (1993).
[21] N. F. Johnson and M. C. Payne, Phys. Rev. B **45**, 3819 (1992).
[22] M. Wagner, U. Merkt, and A. V. Chaplik, Phys. Rev. B **45**, 1951 (1992).
[23] S. R. E. Yang, A. H. Macdonald, and M. D. Johnson, Phys. Rev. Lett. **71**, 3194 (1993).
[24] K. H. Ahn, J. H. Oh, and K. J. Chang, Phys. Rev. B **52**, 13 757 (1995).
[25] A. Yosef, B. Luca, L. Jacob, and R. Roberto, Phys. Rev. E **64**, 056215 (2001).
[26] D. W. Noid, M. L. Koszykowski, and R. A. Marcus, J. Chem. Phys. **71**, 2864 (1971).
[27] D. Farrelly and T. Uzer, J. Chem. Phys. **85**, 308 (1986).